Nanoscale Res Lett (2009) 4:1041–1046
DOI 10.1007/s11671-009-9355-1

NANO EXPRESS

In Situ Mineralization of Magnetite Nanoparticles in Chitosan Hydrogel

Yongliang Wang · Baoqiang Li · Yu Zhou · Dechang Jia

Received: 26 February 2009 / Accepted: 17 May 2009 / Published online: 30 May 2009

Abstract Based on chelation effect between iron ions and amino groups of chitosan, in situ mineralization of magnetite nanoparticles in chitosan hydrogel under ambient conditions was proposed. The chelation effect between iron ions and amino groups in CS–Fe complex, which led to that chitosan hydrogel exerted a crucial control on the magnetite mineralization, was proved by X-ray photoelectron spectrum. The composition, morphology and size of the mineralized magnetite nanoparticles were characterized by X-ray diffraction, Raman spectroscopy, transmission electron microscopy and thermal gravity. The mineralized nanoparticles were nonstoichiometric magnetite with a unit formula of $Fe_{2.85}O_4$ and coated by a thin layer of chitosan. The mineralized magnetite nanoparticles with mean diameter of 13 nm dispersed in chitosan hydrogel uniformly. Magnetization measurement indicated that superparamagnetism behavior was exhibited. These magnetite nanoparticles mineralized in chitosan hydrogel have potential applications in the field of biotechnology. Moreover, this method can also be used to synthesize other kinds of inorganic nanoparticles, such as ZnO, Fe_2O_3 and hydroxyapatite.

Keywords Chitosan hydrogel · Magnetite · Mineralization · Chelation

Y. Wang · B. Li (✉) · Y. Zhou · D. Jia
Institute for Advanced Ceramics, Harbin Institute of Technology, 150001 Harbin, People's Republic of China
e-mail: libq@hit.edu.cn

Y. Wang
e-mail: yongliang@hit.edu.cn

Y. Zhou
e-mail: ce921@hit.edu.cn

Introduction

Mineralization, leading to the formation of minerals in the presence of organic molecules, is a widespread phenomenon in biological system [1, 2]. In the process of mineralization, a small amount of organic component not only reinforces mechanical properties of the resulting materials but also controls the mineralization process, which endows materials with interesting properties such as special crystal morphology and superb mechanical properties [3]. Therefore, mineralization is becoming a valuable approach for novel materials synthesis.

One of the most intriguing examples for mineralization is magnetic bacteria [4, 5]. Each magnetic bacteria acts as a small reaction vessel for mineralization, and the bacterial cell wall can control the iron ions diffusion. Consequently, the magnetite nanoparticles mineralized in magnetic bacteria have perfect shape and size, and the magnetite nanoparticles are assembled into a highly ordered chain structure. Furthermore, the mineralized magnetite nanoparticles in magnetic bacteria are water soluble and biocompatible, which makes it suitable for being used in the fields of bioscience and biomedicine, such as separation for purification and immunoassay [6], drug target delivery [7, 8], magnetic resonance imaging (MRI) [9, 10] and hyperthermia [11]. However, the yield of mineralization of magnetite nanoparticles in magnetic bacteria is too low to make it practical for industrial applications.

Enlightened by the phenomenon of mineralization in magnetic bacteria, a large number of organic molecules have been investigated to realize controllable magnetite mineralization in laboratory. These organic molecules usually contain carboxylic groups [12], sulfate or hydroxyl groups as functional groups [13, 14], which may bind iron ions or control crystal nucleation and growth by lowering the

interfacial energy between the crystal and organic molecules. However, most of these studies focus on the mineralization in solution state that is quite different from the gel state in case of magnetic bacteria. Therefore, researches on mineralization of magnetite in organic hydrogel have great scientific and practical significance.

Inspired by magnetic bacteria, we propose in situ mineralization of magnetite nanoparticles in chitosan hydrogel under ambient conditions. CS–Fe complex was used as a precursor for the mineralization, and the chelation effect of CS–Fe complex can control magnetite mineralization. The mineralized magnetite nanoparticles were well investigated, and the mineralization principle was discussed.

Materials and Methods

Biomedical grade chitosan (viscosity–average molecular weight 3.4×10^5) was supplied by Qingdao Haihui Bioengineering Co., Ltd. with 91.4% degree of the deacetylation. All chemicals were analytical grade reagents and used without further purification.

Preparation of chitosan hydrogel was performed as follows. Three grams of chitosan powder was dissolved in 100 mL of 2% (v/v) acetic acid solution to get 3% chitosan solution. 0.3 mL glutaraldehyde solution (50%) was added to the 100 mL chitosan solution under vigorous stirring to obtain homogeneous solution, in which the molar ratio of aldehyde/amino groups was equal to 1:5. The solution was held until chitosan hydrogel formed completely due to cross-linking effect of glutaraldehyde.

In situ mineralization of magnetite nanoparticles in chitosan hydrogel was carried out as follows. First, the chitosan hydrogel was soaked in 0.15 mol/L $FeCl_3$ solution for 30 min. Then, the chitosan hydrogel with iron ions was washed with deionized water, and soaked in 0.075 mol/L $FeCl_2$ solution for another 30 min. After that, the chitosan hydrogel containing iron ions was subsequently washed with deionized water. This cycle was repeated for 3 times, and the CS–Fe complex was formed. The pH value of the CS–Fe complex was approximately 1.0. Finally, the CS–Fe complex was soaked in NaOH solution (1.25 mol/L) for 12 h, and the magnetite/chitosan composite was achieved. The amount of NaOH was extremely excessive for magnetite mineralization, which induced the concentration of NaOH approximately 1.25 mol/L during the reaction process. Magnetite nanoparticles were obtained after the magnetite/chitosan composite was degraded by H_2O_2, in which the molar ratio of amino/H_2O_2 was equal to 1:2.

X-ray photoelectron spectroscopy (K-Alpha, Thermo Fisher Company) was employed to study interactions between iron ions and chitosan. Crystal structure of mineralized magnetite nanoparticles was investigated by an X-ray diffractometer (D/max-2550, Rigaku) using Cu Kα radiation and a graphite monochromator. The Raman spectra (HORIBA T64000) were excited by 514.5 nm radiation from an argon ion laser. The laser power reaching the sample surface was 20 mW, and the typical acquisition time was 60 s. Transmission electron microscopy (H-7650, Hitachi, Japan) was used to observe the morphology of the magnetite nanoparticles. The mineralized magnetite nanoparticles were also investigated by thermal gravity (STA 449C, Netzsch Company, Germany) to obtain the amount of chitosan layer on the mineralized magnetite nanoparticles. Magnetic properties were determined by Physical Property Measurement System (PPMS-9, Quantum Design, America).

Results and Discussion

CS–Fe Complex

XPS can provide identification of the sorption sites and the interactions between iron ions and chitosan. The XPS spectra of chitosan and CS–Fe complex were shown in Fig. 1. The binding energies for N have a significant change between chitosan and CS–Fe complex. The N 1 s band of chitosan at 397.7 eV was assigned to free amino groups (NH_2), and the band of chitosan at 399.5 eV was attributed to the amino groups that were involved in hydrogen bond (NH_2–O). CS–Fe complex expressed a new band for N 1 s at around 402 eV. This new band was assigned to chelation between the amino groups and iron ions (NH_2–Fe). This chelation effect of CS–Fe complex is the base of mineralization of magnetite in chitosan hydrogel, as demonstrated in this article. Also, XPS can provide the Fe content of the CS–Fe complex, and the Fe content was approximately 2.66 (at.%).

Crystal Structure of the Mineralized Magnetite Nanoparticles

Figure 2 illustrates the XRD patterns for the magnetite/chitosan composite and the mineralized magnetite nanoparticles. In Fig. 2a, the peak at $2\theta = 20.0$ °C was attributed to the presence of chitosan, and it disappeared in Fig. 2b as a result of degradation by H_2O_2. Peaks for magnetite, marked by their indices [(111), (220), (311), (400), (422), (511), (440), (533)], were observed in both curves. No additional peaks were observed.

Even though the peaks matched well with the inverse spinel-structured magnetite, vacancies were inevitable in the crystal because of partial oxidation. In general, non-stoichiometric magnetite can be expressed as $Fe_{3-\delta}O_4$,

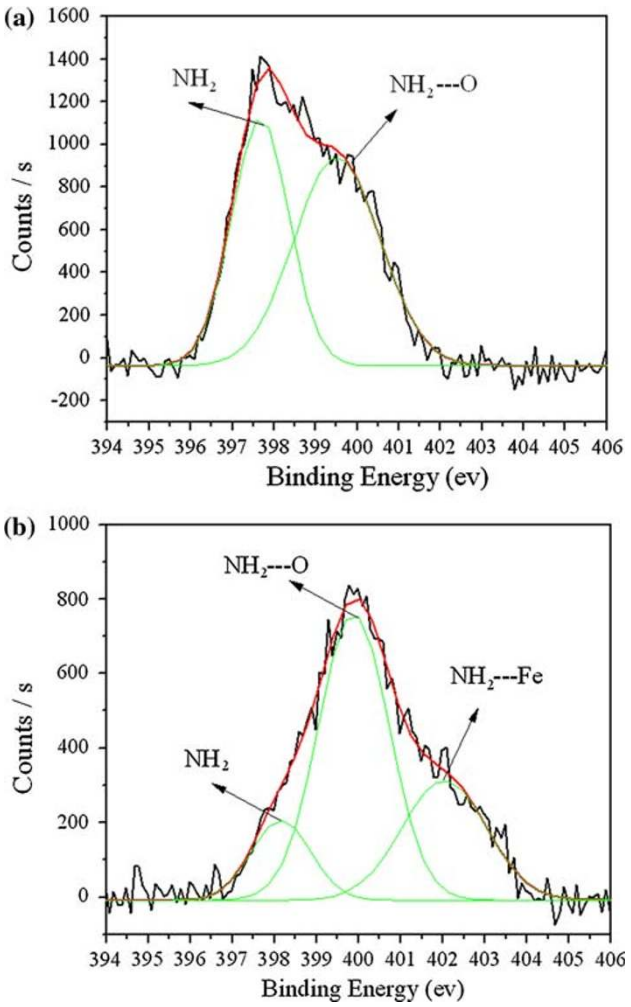

Fig. 1 XPS spectra of chitosan (**a**) and CS–Fe complex (**b**)

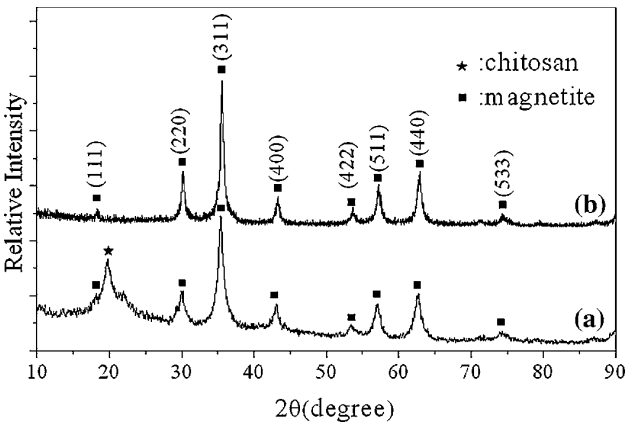

Fig. 2 XRD patterns for the magnetite/chitosan composite (**a**) and the mineralized magnetite nanoparticles (**b**)

where δ is the vacancies number per unit formula. According to Yang's results [15], the unit cell parameter "a" decreased linearly with the increase of δ, and there was a decrease of 0.20 Å in the lattice parameter per vacancy. The calculated unit cell parameter and δ are listed in Table 1, and the unit formulas from curves (a) and (b) are $Fe_{2.91}O_4$ and $Fe_{2.85}O_4$ respectively. Degradation of magnetite/chitosan composite by H_2O_2 caused slight oxidation of mineralized magnetite nanoparticles, which induced a slight increase of δ by 0.06 approximately.

Table 1 The calculated unit formulas of magnetite/chitosan composite and mineralized magnetite nanoparticles

Specimen	2θ (°)	δ	Unit formula ($Fe_{3-\delta}O_4$)	Average
Magnetite/chitosan composite	30.14	0.08	$Fe_{2.92}O_4$	$Fe_{2.91}O_4$
	35.48	0.05	$Fe_{2.95}O_4$	
	43.20	0.13	$Fe_{2.87}O_4$	
	57.10	0.11	$Fe_{2.89}O_4$	
Mineralized magnetite nanoparticles	30.12	0.05	$Fe_{2.95}O_4$	$Fe_{2.85}O_4$
	35.56	0.15	$Fe_{2.85}O_4$	
	43.28	0.20	$Fe_{2.80}O_4$	
	57.26	0.21	$Fe_{2.79}O_4$	

However, because of the similar patterns between Fe_3O_4 and γ-Fe_2O_3, the XRD patterns cannot provide enough evidences to confirm that the mineralized nanoparticles were magnetite. Raman spectroscopy was used to characterize the mineralized nanoparticles, and the Raman spectrum is revealed in Fig. 3a. The mineralized nanoparticles showed a peak around 667 cm^{-1}, which was in agreement with the reported typical value of magnetite in the literature (660 cm^{-1} [16]). For comparison purposes, the Raman spectrum of γ-Fe_2O_3 was illustrated in Fig. 3b, and three broad peaks around 350, 500 and 700 cm^{-1} were observed. No peak around 667 cm^{-1} appears in Fig. 3b. The Raman spectrum, combined with the XRD patterns, indicated that the mineralized nanoparticles were exactly nonstoichiometric magnetite, rather than γ-Fe_2O_3.

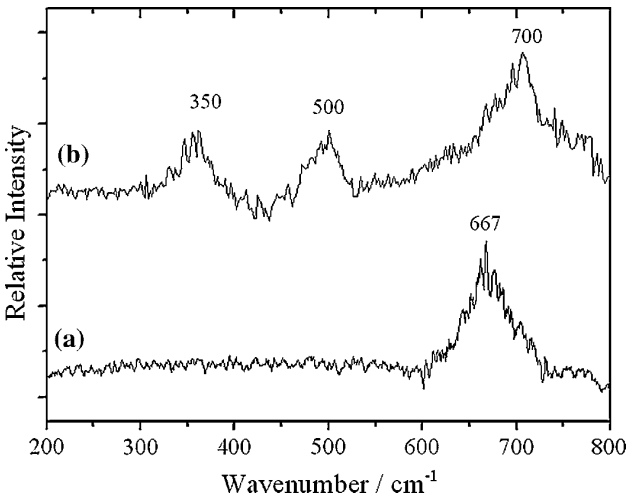

Fig. 3 The Raman spectra of mineralized magnetite nanoparticles (**a**) and γ-Fe_2O_3 (**b**)

Morphology of the Mineralized Magnetite Nanoparticles

The magnetite/chitosan composite was treated with ultra thin cutting to observe the dispersion of magnetite nanoparticles in magnetite/chitosan composite (Fig. 4a). Also, the morphology of magnetite nanoparticles was shown (Fig. 4b) after the magnetite/chitosan composite was degraded by H_2O_2. As can be seen from Fig. 4a, the magnetite nanoparticles with mean diameter of 13 nm (statistical result illustrated in Fig. 4d) dispersed in the chitosan hydrogel uniformly. Compared with literatures [17, 18], the mineralized magnetite nanoparticles in this work have characters of smaller diameter and narrow size distribution. The reason for uniform dispersion and narrow size distribution might be that the moving ability of iron ions in the chitosan hydrogel is low, which avoided abnormal growth of magnetite grains. Selected area electron diffraction (SAED) pattern from Fig. 4a was shown in Fig. 4c, and it was confirmed that the nanoparticles were exactly magnetite.

As can be seen in Fig. 4b, there was a blurred layer coating on the Fe_3O_4 nanoparticles. It is believed that the blurred layer could be assigned to chitosan layer on mineralized magnetite nanoparticles.

Chitosan Layer on the Mineralized Magnetite Nanoparticles

Considering the chelation effect between iron ions and amino groups in CS–Fe complex, the mineralized magnetite nanoparticles were inevitably coated by a thin layer of chitosan. Moreover, the TEM morphology of mineralized magnetite nanoparticles proved the existence of chitosan layer. In order to obtain the amount of chitosan layer on the mineralized magnetite nanoparticles, the mineralized magnetite nanoparticles were analyzed by TG, and the result is displayed in Fig. 5. For comparison, TG curve of pure magnetite without chitosan is also illustrated.

As can be seen in Fig. 5a, in the interval of 200–800 °C, there was no weight loss for pure magnetite. However, the mineralized magnetite nanoparticles experienced a 19.1% weight loss that was assigned to the decomposition of acetylated and deacetylated units of chitosan layer coating on mineralized magnetite nanoparticles (Fig. 5b). The

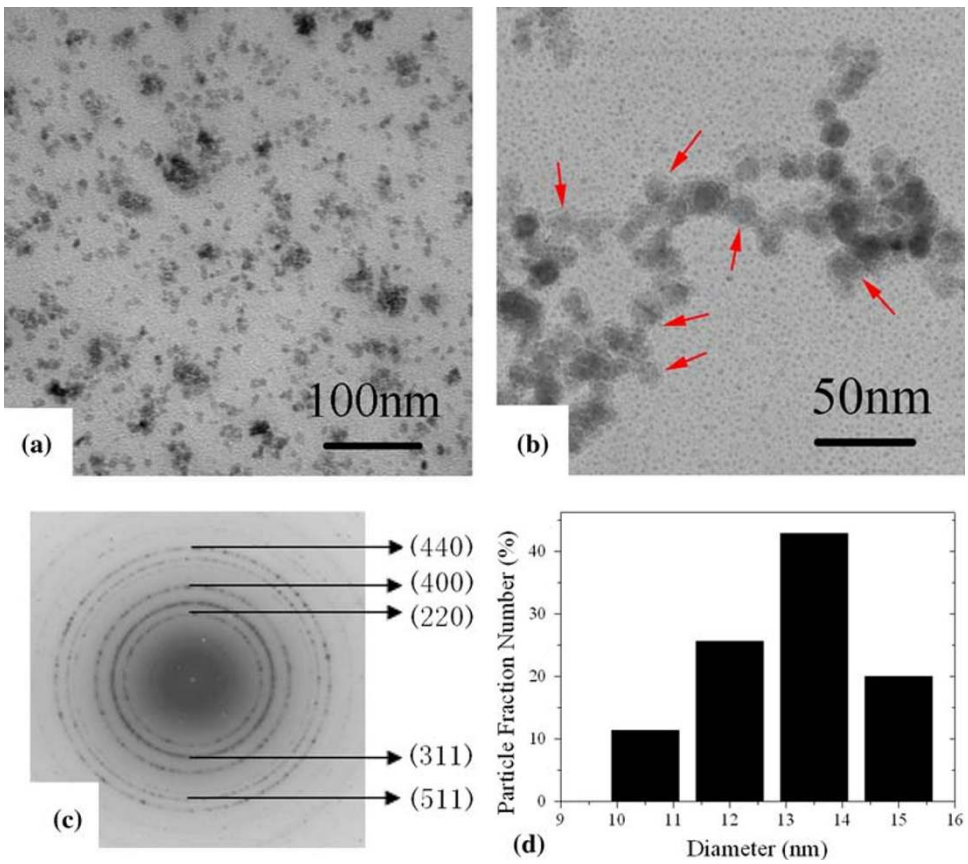

Fig. 4 TEM morphologies of magnetite/chitosan composite (**a**) and mineralized magnetite nanoparticles (**b**); selected area electron diffraction (*SAED*) pattern (**c**) and statistical result of magnetite nanoparticle size distribution from Fig. 4a (**d**)

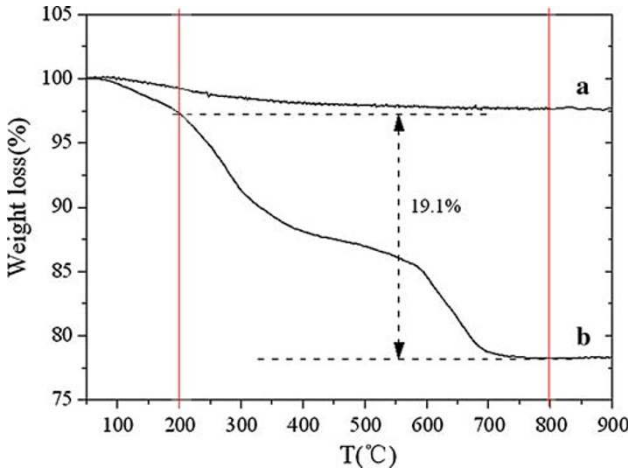

Fig. 5 TG curves of pure magnetite (**a**) and the mineralized magnetite nanoparticles (**b**)

existence of chitosan layer changes the properties of magnetite nanoparticles and makes it water soluble and biocompatible, which makes it has potential applications in the field of biotechnology as magnetic resonance imaging contrast agents and drug carrier.

Magnetic Properties of the Mineralized Magnetite Nanoparticles

Figure 6 shows the hysteresis loop of mineralized magnetite nanoparticles at 300 K. As can be seen in Fig. 6, the saturated magnetization (Ms) of mineralized magnetite nanoparticles was 51.6 emu/g, which was as high as 56% of bulk magnetite (92 emu/g). The remanence (Mr) and coercivity (Hc) of the mineralized magnetite nanoparticles were 0.9 emu/g and 16.5 Oe, respectively. As described in Yaacob's literature [19], an estimate of the upper bound for magnetite particle size can be obtained from the slope of the magnetization near zero field. The calculated result for d_{max} is 17.9 nm, that is consistent with the statistical result from TEM.

Principle of In Situ Mineralization of Magnetite in Chitosan Hydrogel

The principle of magnetite mineralization in chitosan hydrogel was similar to that of mineralization in magnetic bacteria. The pore in chitosan hydrogel acts as a reaction vessel. As a result of chelation effect, the amino groups can control the iron ions diffusion during mineralization. The principle of magnetite mineralization in chitosan hydrogel is illustrated in Fig. 7. Firstly, iron ions were chelated by the amino groups of chitosan, and the CS–Fe complex was fabricated. When the CS–Fe complex encountered OH^-, the ferric and ferrous ions chelated by the amino groups [$(\text{chitosan-NH}_2)_2$–Fe^{2+}, $(\text{chitosan-NH}_2)_2$–Fe^{3+}] provided nucleation site for magnetite crystals. Then, crystal growth of magnetite was controlled by iron ions diffusion, which was restricted by the chelation effect. Considering the random dispersion of amino groups in chitosan hydrogel, the iron ions can only move to the nearest magnetite nucleus, which avoided abnormal growth of magnetite grains. In view of these reasons, the mineralized magnetite nanoparticles in chitosan hydrogel have a narrow size distribution and small diameter.

Conclusions

In situ mineralization of magnetite nanoparticles in chitosan hydrogel under ambient conditions was proposed. The chelation effect between iron ions and amino groups in CS–Fe complex was proved by XPS. The mineralized magnetite nanoparticles, which were coated by chitosan layer, have a narrow size distribution and small diameter.

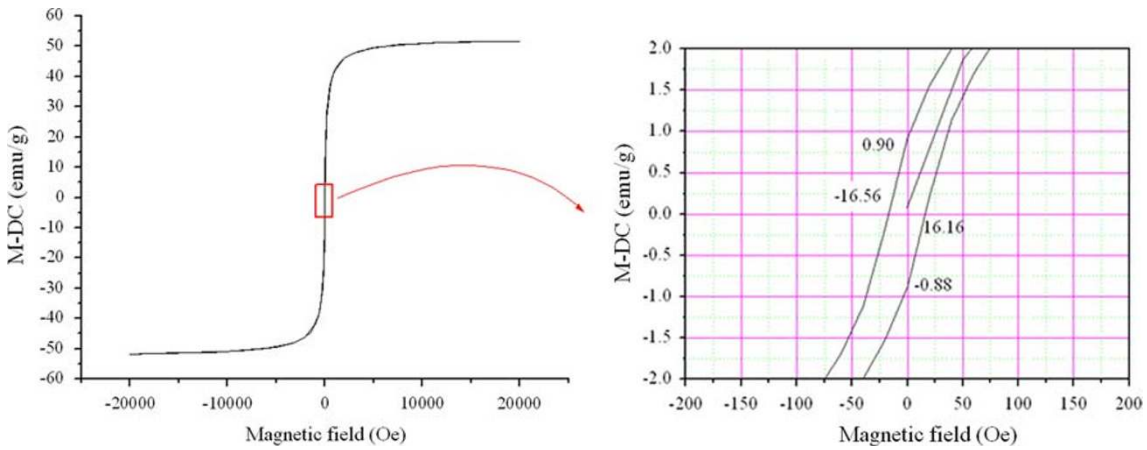

Fig. 6 Hysteresis loop of the mineralized magnetite nanoparticles at 300 K

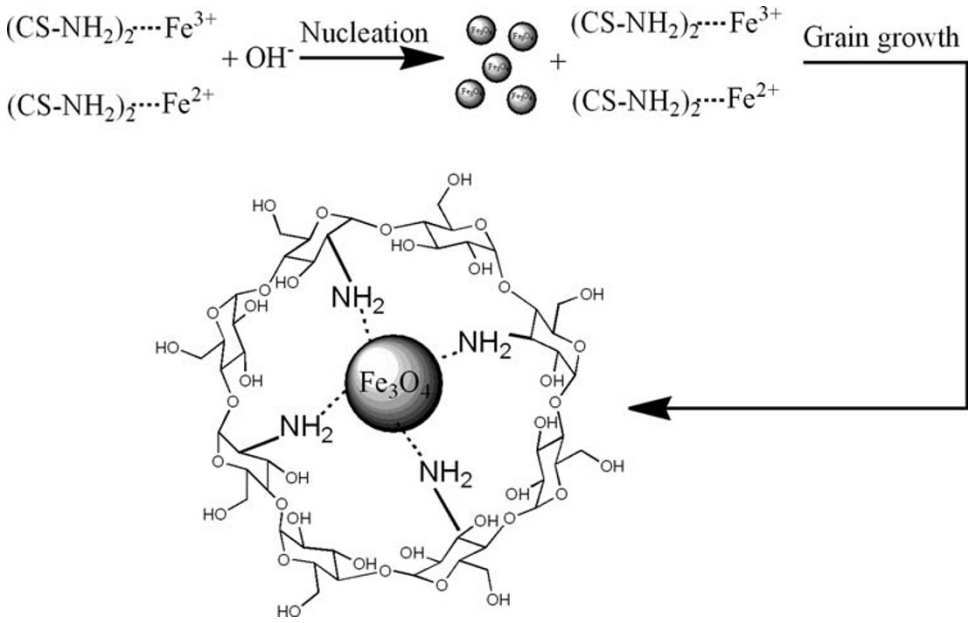

Fig. 7 Principle of in situ mineralization of magnetite nanoparticles in chitosan hydrogel

XRD analysis and Raman spectra indicated that the mineralized nanoparticles were nonstoichiometric magnetite and the unit formula was $Fe_{2.85}O_4$. The mineralized magnetite nanoparticles with a mean diameter of 13 nm dispersed in chitosan hydrogel uniformly. Magnetization measurement indicated that superparamagnetism behavior was shown and the coercitivity and the remanence were 16.5 Oe and 0.9 emu/g respectively. The principle of magnetite mineralization in chitosan hydrogel can be expatiated as follows. First, iron ions were chelated by the amino groups of chitosan, and the CS–Fe complex was fabricated. When the CS–Fe complex encountered OH^-, the iron ions chelated by the amino groups, which providing nucleation site for magnetite crystals. The iron ions diffusion was restricted by chelation effect, and abnormal crystal growth of magnetite was avoided; thus, magnetite nanoparticles with small diameter and narrow size distribution were formed.

Acknowledgments The authors thank the financial support from National Science Foundation of China (50702017), the Innovation Foundation of Harbin Institute of Technology (HIT. NSRIF. 2008.51) the Post-Doctor Foundation (20060390786), and the program of excellent team in Harbin Institute of Technology.

References

1. A.W. Xu, Y.R. Ma, H. Colfen, J. Mater. Chem. **17**, 415 (2007). doi:10.1039/b611918m
2. G. Fu, S.R. Qiu, C.A. Orme, D.E. Morse, J.J. De Yoreo, Adv. Mater. **17**, 2678 (2005). doi:10.1002/adma.200500633
3. M. Hildebrand, Chem. Rev. **108**, 4855 (2008). doi:10.1021/cr078253z
4. D. Faivre, D. Schuler, Chem. Rev. **108**, 4875 (2008). doi:10.1021/cr078258w
5. A.A. Bharde, R.Y. Parikh, M. Baidakova, S. Jouen, B. Hannoyer, Langmuir **24**, 5787 (2008). doi:10.1021/la704019p
6. H.W. Gu, K.M. Xu, C.J. Xu, B. Xu, Chem. Commun. (Camb.) **6**, 941 (2006). doi:10.1039/b514130c
7. K. Landfester, L.P. Ramirez, J. Phys, Condens. Matter. **15**, S1345 (2003). doi:10.1088/0953-8984/15/15/304
8. S.X. Wang, Y. Zhou, W. Guan, B.J. Ding, Nanoscale Res. Lett. **3**, 289 (2008). doi:10.1007/s11671-008-9151-3
9. H.S. Lee, H.P. Shao, Y.Q. Huang, B.K. Kwak, IEEE Trans. Magn. **41**, 4102 (2005). doi:10.1109/TMAG.2005.855338
10. S.A. Corr, Y.P. Rakovich, Y.K. Gun'ko, Nanoscale Res. Lett. **3**, 87 (2008). doi:10.1007/s11671-008-9122-8
11. D.H. Kim, K.H. IM, S.H. Lee, K.N. Kim, K.M. Kim, K.D. Kim, H. Park, I.B. Shim, Y.K. Lee, IEEE Trans. Magn. **41**, 4158 (2005). doi:10.1109/TMAG.2005.854857
12. A. Bee, R. Masssart, S. Neveu, J. Magn. Magn. Mater. **149**, 6 (1995). doi:10.1016/0304-8853(95)00317-7
13. A.L. Daniel-da-Silva, T. Trindade, B.J. Goodfellow, B.F.O. Costa, R.N. Correia, A.M. Gil, Biomacromolecules **8**, 2350 (2007). doi:10.1021/bm070096q
14. E. Kroll, F.M. Winnik, Chem. Mater. **8**, 1594 (1996). doi:10.1021/cm960095x
15. J.B. Yang, X.D. Zhou, W.B. Yelon, W.J. James, Q. Cai, X.C. Sun, D.E. Nikles, J. Appl. Phys. **95**, 7540 (2004). doi:10.1063/1.1669344
16. D.L.A. de Faria, S.V. Silva, M.T. de Oliveira, J. Raman Spectrosc. **28**, 873 (1997). doi:10.1002/(SICI)1097-4555(199711)28:11<873::AID-JRS177>3.0.CO;2-B
17. S.Y. Gao, Y.G. Shi, S.X. Zhang, K. Jiang, S.X. Yang, Z.D. Li, E. Takayama-Muromachi, J. Phys. Chem. C **112**, 10398 (2008). doi:10.1021/jp802500a
18. G.Y. Li, Y.R. Jiang, K.L. Huang, P. Ding, J. Chen, J. Alloy Comp. **466**, 451 (2008). doi:10.1016/j.jallcom.2007.11.100
19. I.I. Yaacob, A.C. Nunes, A. Bose, J. Colloid Interface Sci. **171**, 73 (1995). doi:10.1006/jcis.1995.1152